Journal of Power Sources 196 (2011) 1626–1631

Contents lists available at ScienceDirect

Journal of Power Sources

journal homepage: www.elsevier.com/locate/jpowsour

Polyfluorinated boron cluster based salts: A new electrolyte for application in nonaqueous asymmetric AC/$Li_4Ti_5O_{12}$ supercapacitors

C.M. Ionica-Bousquet[a,*,1], D. Muñoz-Rojas[a,*,2], W.J. Casteel Jr.[b], R.M. Pearlstein[b], G. Girish Kumar[b], G.P. Pez[b], M.R. Palacín[a]

[a] Institut de Ciència de Materials de Barcelona, CSIC, Campus UAB, E-08193 Bellaterra, Spain
[b] Air Products and Chemicals, Inc., 7201 Hamilton Blvd., Allentown, PA 18195, USA

ARTICLE INFO

Article history:
Received 12 July 2010
Received in revised form 20 August 2010
Accepted 25 August 2010
Available online 28 September 2010

Keywords:
Redox active electrolytes
Hybrid cells
Batteries
Asymmetric supercapacitors
Overcharge protection
Polyfluorinated boron cluster

ABSTRACT

Solutions of novel fluorinated lithium dodecaborate ($Li_2B_{12}F_xH_{12-x}$) salts have been evaluated as electrolytes in nonaqueous asymmetric supercapacitors with $Li_4Ti_5O_{12}$ as negative electrode, and activated carbon (AC) as positive electrode. The results obtained with these new electrolytes were compared with those obtained with cells built using standard 1 M $LiPF_6$ dissolved in ethylene carbonate and dimethyl carbonate (EC:DMC; 1:1, v/v) as electrolyte. The specific energy, rate capability, and cycling performances of nonaqueous asymmetric cells based on these new electrolyte salts were studied. Cells assembled using the new fluoroborate salts show excellent reversibility, coulombic efficiency, rate capability and improved cyclability when compared with the standard electrolyte. These features confirm the suitability of lithium-fluoro-borate based salts to be used in nonaqueous asymmetric supercapacitors.

1. Introduction

Research efforts on electrochemical capacitors are directed at increasing the energy density, as well as lowering fabrication costs, while using environmentally friendly materials. An interesting approach has been to develop hybrid systems that typically consist of an electrochemical-double layer capacitor electrode and a battery-like one, thereby having a potential to deliver both high power density and high energy density.

The concept of nonaqueous asymmetric supercapacitors was introduced by Amatucci and co-workers [1–3] using anodes based on $Li_4Ti_5O_{12}$ and either carbon or conducting polymer cathodes in a nonaqueous electrolyte ($LiPF_6$ dissolved in a organic solvent such as acetonitrile, propylene carbonate, etc.), thus enabling high voltage operation. In such a system the negative electrode supports the fast intercalation of lithium ions, while the positive electrode stores charge by a reversible non-faradaic or pseudocapacitive mechanism through the formation of the double layer on the surface of the carbon electrode. Activated carbons having a high surface area have been typically used as one of the electrodes in combination with different lithium intercalation compounds that have been used either as the positive, e.g. $LiMn_2O_4$ [4], $LiCo_{1/3}Ni_{1/3}Mn_{1/3}O_2$, $LiCoO_2$ [5]; or as the negative, e.g. TiO_2 [6] and $Li_4Ti_5O_{12}$ [1,7] counter electrode.

These devices are of great interest for systems requiring fast charge/discharge rates while keeping a reasonable energy density where they can find applications both in consumer electronics (e.g., fast charge of portable phones) and in automotive devices [6,8]. The concept of an asymmetric supercapacitor, already demonstrated at the fundamental level, is now in its development and pre-commercialization phase, large prototypes having already been developed and tested by Telcordia [8].

Recently, polyfluorinated boron cluster salts, i.e. lithium polyfluorododecaborates ($Li_2B_{12}F_xZ_{12-x}$ where $x \leq 12$ and Z = H, Cl or Br) [9,10] have been developed and tested as electrolyte salts both in Li-ion batteries [11] and nonaqueous supercapacitors [12]. The advantages associated to the use of these new electrolytes include: high electrochemical, thermal, and hydrolytic stability. Another key feature of these salts is their ability to provide intrinsic protection against overcharge through a redox-shuttle chemistry [10], which in the case of supercapacitors translates in an extension of the cell life when it is subjected to harsh conditions [12].

Here we present a study of two of these new boron cluster based salts, namely $Li_2B_{12}F_{12}$ and a mixture having average

* Corresponding author. Tel.: +44 1223334374; fax: +44 1223334375.
E-mail addresses: costana.bousquet@univ-montp2.fr (C.M. Ionica-Bousquet), davidmunozrojas@gmail.com (D. Muñoz-Rojas).
[1] Present address: AIME-ICG, Université Montpellier II, CC1502, Place E. Bataillon, 34095 Montpellier Cedex 5, France.
[2] Present address: Department of Materials Science and Metallurgy, University of Cambridge, Pembroke St, Cambridge CB2 3QZ, UK.

0378-7753/$ – see front matter © 2010 Elsevier B.V. All rights reserved.
doi:10.1016/j.jpowsour.2010.08.082

composition $Li_2B_{12}F_8H_4$, as possible electrolytes in nonaqueous asymmetric supercapacitors using $Li_4Ti_5O_{12}$ as negative electrode in combination with AC positive electrode. Their stability, cyclability and capacity retention have been studied and compared to those obtained with standard $LiPF_6$ electrolyte as reference.

2. Experimental

2.1. Electrode materials

Activated carbon (Fluka) denoted AC hereafter, was used as positive electrode while $Li_4Ti_5O_{12}$ to be used as negative electrode was prepared as reported elsewhere [13,14] from TiO_2 (<5 μm, 99.9%, Aldrich) and Li_2CO_3 (99%, Aldrich). The starting materials were dispersed in a solution of alcohol/deionized water/sugar (99%, Alfa Aesar) (weight ratio: 3.3:1.3:1) and after removing the solvent, the resulting powder was ground and heat-treated in air at 750 °C for 12 h to decompose Li_2CO_3 and then at 850 °C for 24 h. The phase purity of the resulting powders was checked by X-ray powder diffraction (XRD) using a Rigaku Rotaflex Ru-200B Spectrometer with Cu Kα radiation source (λ = 1.5418 Å). Cell parameters were refined with the program FULLPROF [15]. Grain morphology and particle size were determined by scanning electronic microscopy (SEM) using a Philips 515 with 5 nm resolution which can be operated between 0.2 and 30 kV. Specific surface areas were evaluated by N_2 gas adsorption and desorption measurements (Micrometrics ASAP 2000) using the Brunauer–Emmett–Teller (BET) method.

2.2. Cell assembly

Most electrochemical experiments were made using two-electrode Swagelok™ cells [16]. In all cases, identical cells were assembled and tested at the same time using the new salts as well as $LiPF_6$ as reference. Additional experiments were carried out in three-electrode cells, using lithium metal as reference electrode, thus allowing the measurement of the potential of both the positive and negative electrodes independently during cell operation.

$Li_4Ti_5O_{12}$ electrodes were fabricated by doctor blade casting of a slurry containing 84 wt% oxide powder, 8% acetylene black powder and 8 wt% binder (polyvinylidene difluoride, PVDF) dissolved in N-methylpyrrolidone (NMP) onto the current collector (18 μm thick copper foil, GoodFellow). Disk shaped electrodes having a 0.95 cm^2 area were punched out and dried at 120 °C under vacuum prior to use. The typical loading of active material was in the range of 3–5 mg cm^{-2} while the thickness of the dried electrodes was 15–20 μm.

Self-standing AC electrodes were prepared using polytetrafluoroethylene, PTFE, as binder. A paste was prepared by mixing 85 wt% AC, 10 wt% SP Carbon powder (kindly supplied by MMM, Belgium) and 5 wt% PTFE (60% PTFE dispersed in water, Aldrich) that was spread into 5 cm × 10 cm sheets about 35 μm thick from which 0.95 cm^2 circular electrodes were cut. The electrodes were also dried at 120 °C in vacuum prior to use. The typical loading of active material was in the range of 20–30 mg cm^{-2}.

Two sheets of Whattman GF/D borosilicate glass fiber soaked with electrolyte were used as separator. Three electrolyte solutions were used: 0.4 M $Li_2B_{12}F_{12}$ in ethylene carbonate/dimethylcarbonate (EC/DMC 1:1 volume), 0.4 M $Li_2B_{12}F_8H_4$ in EC/DMC (1:1 volume) and 1 M $LiPF_6$ in EC/DMC (1:1 volume; Merck Battery Grade), denoted hereafter 'BF', 'BFH' (new salts evaluated in this study) and 'LP30', respectively. The two electrolyte salts, $Li_2B_{12}F_{12}$ and $Li_2B_{12}F_8H_4$, were prepared and purified as reported elsewhere [9].

The positive and negative electrodes active material weight ratio was close to 4:1. This balancing ratio was calculated considering 120 mAh g^{-1} specific capacity for $Li_4Ti_5O_{12}$ and 30 mAh g^{-1} specific capacity for AC, as reported previously [17]. The specific capacity of the cells and the electrochemical rate were always referred to the total weight of the electrode materials, including the positive and the negative electrodes. The cells were charged and discharged at room temperature, at various rates, between 10 and 150C, using a VMP Potentiostat/Galvanostat (Bio-Logic) operating in a galvanostatic mode. The voltage operation window, 1.2–3 V, was chosen after reference [17]. Longer tests to assess cycle life were also performed in a wider voltage window, i.e. between 1.0 and 3.5 V. Finally, a conventional AC/AC supercapacitor was assembled and tested using the BFH electrolyte for comparative purposes.

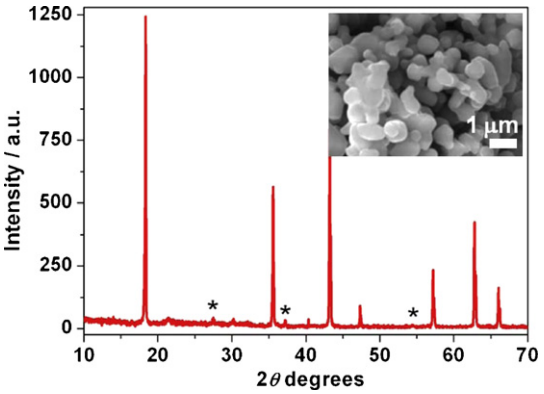

Fig. 1. XRD pattern and SEM micrographs (inset) of the $Li_4Ti_5O_{12}$ spinel prepared for this study. The black stars denote diffraction lines from rutile TiO_2 impurity phase.

3. Results and discussion

3.1. Materials characterization

The XRD pattern of the as prepared $Li_4Ti_5O_{12}$ sample is shown in Fig. 1. The main diffraction peaks of the $Li_4Ti_5O_{12}$ spinel phase are present along with some minor extra diffraction peaks at $2\theta = 27.4°$, 37.3° and 54.3° that are attributed to the presence of a small amount of rutile TiO_2 impurities. The refined cell parameter for $Li_4Ti_5O_{12}$ is $a = 0.83562(2)$ nm, which is in good agreement with that reported by Ohzuku et al. [18]. A typical SEM micrograph is shown in the inset in Fig. 1 in which regular 0.8–1 μm particles can be seen. BET measurements indicate a surface area of 8 $m^2\ g^{-1}$ and absence of porosity in the micrometer range. The synthesis method used allows the preparation of homogeneous compounds with finer particle size due to the decomposition of the sugar added during the heat-treatment which inhibits particle agglomeration [13,14].

Table 1 lists the characteristics of the Fluka activated carbon, a highly porous material which exhibits high surface area (1078 $m^2\ g^{-1}$).

3.2. Electrochemical performance

In order to follow the voltage evolution of the individual electrodes during galvanostatic charge/discharge at constant rate, cycling was performed for one asymmetric supercapacitor containing BF electrolyte assembled using a three-electrode cell. Fig. 2 shows the profiles of the charge/discharge curves for the $Li_4Ti_5O_{12}$

Table 1
BET surface area and pore size distribution obtained by the BJH (Barrett–Joyener–Halenda) method.

BET Surface ($m^2\ g^{-1}$)	1078.4
Micropore area ($m^2\ g^{-1}$)	676.9
Microporous volume <20 Å ($cm^3\ g^{-1}$)	0.4
Average pore diameter adsorption (nm)	5.15
Average pore diameter desorption (nm)	4.42

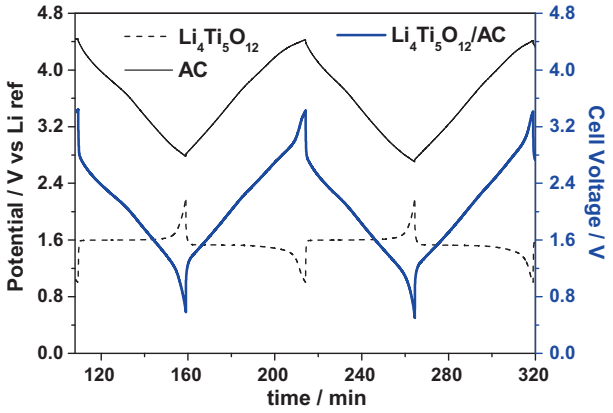

Fig. 2. Charge–discharge curves of the individual $Li_4Ti_5O_{12}$ and AC electrodes along with a composite voltage profile of a nonaqueous asymmetric $Li_4Ti_5O_{12}$/AC supercapacitor assembled using $Li_2B_{12}F_{12}$ (BF) electrolyte tested in a three-electrode cell at 2C constant charge/discharge rate using lithium metal as reference electrode.

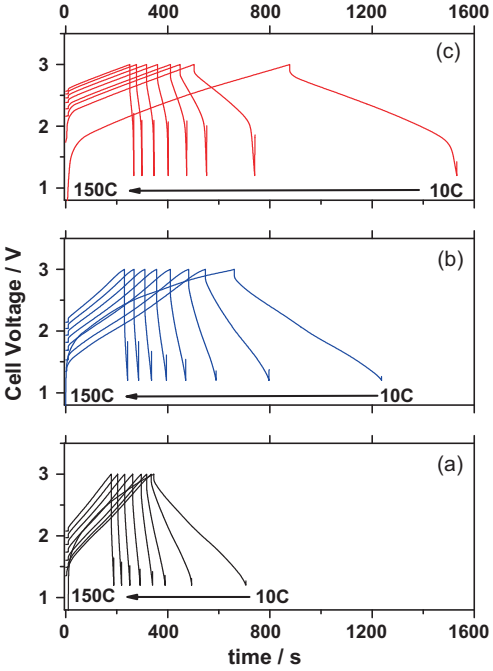

Fig. 3. Charge–discharge curves of three asymmetric cells at different rates (10, 20, 40, 60, 80, 100, 120 and 150C): (a) AC/BF/$Li_4Ti_5O_{12}$, (b) AC/BFH/$Li_4Ti_5O_{12}$, and (c) AC/LP30/$Li_4Ti_5O_{12}$.

and AC electrodes, as well as the voltage profile of the entire nonaqueous asymmetric system. It can be noted that the cycling profile of the hybrid obtained using the three electrodes configuration is similar to the one obtained when using the two-electrode cell (cf. Fig. 3). The observed voltage profile of the $Li_4Ti_5O_{12}$ electrode is equivalent to the one previously obtained in Li-ion batteries [11] built with the same electrolyte and is consistent with the well-known insertion mechanism involving a phase transition. Thus, during the discharge the voltage quickly drops down to below 1.8 V and decreases to a value about 1.55 V, after which the voltage profile has a flat operating voltage at about 1.50–1.55 V vs Li^+/Li^0 corresponding to the reversible two-phase transition plateau. On the other hand, the active carbon presents the typical linear charge–voltage behavior found in EDLC electrodes, consistent with previous reports on asymmetric systems [5].

3.2.1. Rate capability

Electrochemical characterization of the AC/$Li_4Ti_5O_{12}$ cells was performed in galvanostatic mode at constant charge rate (10C) and different discharge rates (varying from 10 to 150C). Table 2 summarizes the discharge rate, current density, first cycle discharge capacity, first cycle irreversible capacity and efficiency after 10 cycles obtained for the cells made with the three electrolytes. The discharge rate was increased every 10 cycles. For each of the rates used, the efficiency over 10 cycles was calculated taking into account the first discharge capacity as reference.

Fig. 3 shows the profiles of the first charge/discharge curves at the different rates tested (current density varying from 1.3 to 36 mA cm^{-2}) for the cells listed in Table 2. It is important to notice that the cells built using BF and BFH electrolytes exhibit much better performances: small first cycle irreversibility (8–12%, com-

Table 2
Summary of the electrochemical performance of the cells assembled with the three electrolytes.

Electrolyte	Discharge rate	Current densities (mA cm^{-2})	1st discharge capacity (mAh g^{-1})	1st cycle loss (%)	10 cycles efficiency (%)
BF	10C	2.4	12.7	7.6	99.9
	20C	4.8	12.7	3.3	95.7
	40C	9.5	11.5	5.6	95.5
	60C	14.3	10.3	7.2	93.9
	80C	19.0	8.8	9.3	93.3
	100C	23.4	7.4	10.9	94.0
	120C	28.5	6.6	5.5	95.1
	150C	35.7	6.2	1.0	96.0
BFH	10C	1.7	15.4	12.5	89.0
	20C	3.3	13.3	8.2	91.1
	40C	6.7	11.4	9.2	90.9
	60C	10.0	9.6	9.7	93.7
	80C	13.4	8.2	10.9	94.8
	100C	16.7	7.0	12.8 15.1	96.4
	120C	20.0 25.1	5.8	19.9	99.0
	150C		4.7		97.7
LP30	10C	1.3	20	25.2	74.4
	20C	2.6	14.5	4.5	91.3
	40C	5.1	12.7	5.4	95.8
	60C	7.7	11,6	9.8	91.6
	80C	10.2	10.2	5.0	91.4
	100C	12.8	8.9	5.2	91.6
	120C	15.4 19.2	7.8	5.5	94.9
	150C		6.9	7.4	91.8

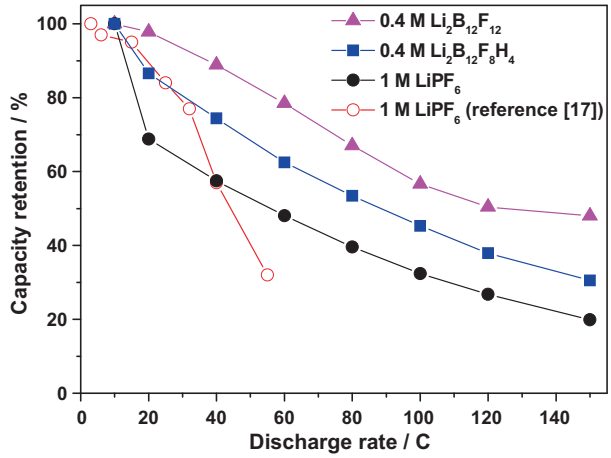

Fig. 4. Comparison of the capacity retention obtained for cells assembled using $Li_2B_{12}F_{12}$ (BF), $Li_2B_{12}F_8H_4$ (BFH) and $LiPF_6$ (LP30) electrolytes. Data from Ref. [17] are included for comparison.

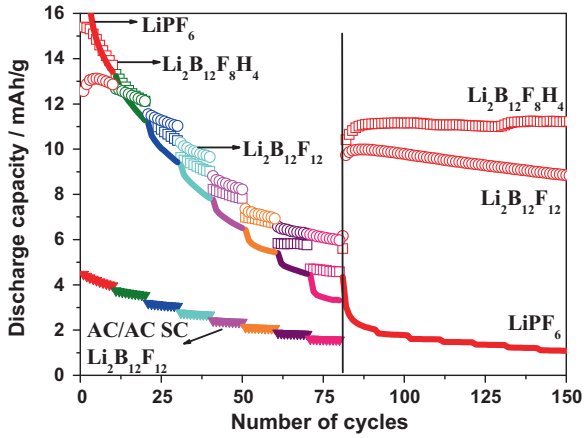

Fig. 5. Discharge capacity vs. cycle number for cells with $Li_2B_{12}F_{12}$ (BF), $Li_2B_{12}F_8H_4$ (BFH) and $LiPF_6$ (LP30) electrolytes at constant charge rate (10C) and various discharge rates, up to 150C (first 80 cycles) and then back to 10C discharge rates (last 70 cycles). The results obtained for a symmetric supercapacitor with two AC electrodes and BF electrolyte are also shown for comparison (only the first 80 cycles).

pared to 25% for LP30) and improved efficiency. For the 10C/10C charge/discharge rate the efficiency over 10 cycles was close to 100% for the cell with BF electrolyte, 89% for the one with BFH electrolyte, and 74% for the standard using LP30. Even at high cycling rate the cells built using the new fluorinated lithium dodecaborate electrolytes exhibit increased efficiency with respect to LP30 standard, with BF showing the best results.

The capacity retention at various rates was calculated by taking the capacity at 10C as reference. Fig. 4 exhibits the plot of capacity retention versus the discharge rate with the $Li_4Ti_5O_{12}$ electrode. The discharge capacities for the cells containing boron cluster based salts are compared with those obtained for LP30. For comparative purposes, literature data reported for a AC/LP30/LTO cell (with similar particle size for the negative electrode material), charged at 3C and discharged at various current rates, varying from 3 to 55C, is also included.

The cells assembled with boron cluster based salt electrolytes exhibit much better cyclability, as compared to the standard LP30 and to the electrolyte used in Ref. [17], i.e., 1 M $LiPF_6$ ethylene carbonate (EC)/ethylene methyl carbonate (EMC)/dimethyl carbonate (DMC) (1:1:1, v/v). Although the capacity values decrease at very fast discharge rates, the calculated capacity retention at 150C rate is 48% for BF and 31% for BFH, while the cell using LP30 exhibits only 20%. The latter exhibits a much larger fading at high discharge rates, the capacity retention at 40C already being the 57% only, while BF and BFH electrolytes retained a 89% and a 75%, respectively, in the same conditions.

3.2.2. Ability to recover capacity after high rate cycling

As shown in Fig. 5, only the cells assembled with the new fluorinated lithium electrolytes succeed in recovering a capacity comparable to the one initially delivered at a 10C constant cycling rate. High cycling rate operation (>140C) does not seem to damage these cells, since the original performance is recovered when lower rates are reimposed (10C). The efficiency over 150 cycles (80 cycles at various discharge rates plus 70 at constant 10C rate) was also calculated, referencing against the first cycle discharge. The obtained values are very similar, 64% efficiency for both BF and BFH cells, while only 3% is achieved for LP30, confirming the much better stability of polyfluorinated boron cluster salts.

Furthermore, the same electrochemical protocol (galvanostatic charge at constant rate/discharge at various rates) was applied to a symmetric AC/AC cell with BF electrolyte and the results are compared with those obtained for the asymmetric cells (Fig. 4). The discharge rate was increased every 10 cycles. The asymmetric cells present improved capacity values when compared to the AC/AC cell, especially at lower rates where most of the $Li_4Ti_5O_{12}$ Li intercalation capacity can be harnessed.

3.2.3. Long term cycling behavior

The long term cycling ability of the cells under study was also examined by constant 10C rate charge/discharge cycling, between 1.2 and 3 V.

As shown in Fig. 6a, which reports the capacity retention of the cells under study after 1000 cycles, the cells using BF and BFH electrolytes exhibit better performance: higher capacity and improved stability. After 1000 cycles, the calculated capacity losses were: 37% for the cell with BF, 72% for the one with BFH and 98% for the standard LP30. Under these specific cycling conditions, the cell assembled using the $Li_2B_{12}F_{12}$ salt (BF) presents the best performance. For this electrolyte-based device an "activation" process seems to take place during the first 20 cycles wherein an initial capacity loss is observed, but after which the delivered capacity is relatively stable.

In order to study the influence of the voltage window on the electrochemical performance of the cells in terms of capacity and stability upon cycling, experiments were also carried out between 1 and 3.5 V (Fig. 6b). After 1000 cycles, the calculated capacity losses were: 65% for the cell with BF, 50% for the one with BFH and 95% for LP30. An important improvement of the reversible capacity and stability of the cell built using BFH electrolyte device was thus obtained by increasing the potential test window from 1.2–3 to 1–3.5 V, probably due to the protective contribution of the redox couple of $Li_2B_{12}F_8H_4$ to the electrochemical process. A 210% gain in capacity was calculated considering that the capacity obtained after 1000 cycles between 1.2 and 3 V is the maximum value that can be obtained on charge. Increasing the width of the test voltage window, however, did not seem to improve that much the relative performance of the cell built using BF electrolyte. On the other hand, the cell made with the standard LP30 showed a dramatic decrease in performance due to the increase in voltage window, with capacity fading very abruptly during the initial 50 cycles (Fig. 6b). As we have shown previously [11,12], both batteries and supercapacitors built with the novel salt electrolytes show a huge increase in stability which is due to the protective shuttle effect conferred by the active redox pair present in the salt anion. In the case of the hybrid cells, the redox activity of the electrolyte again plays a main role

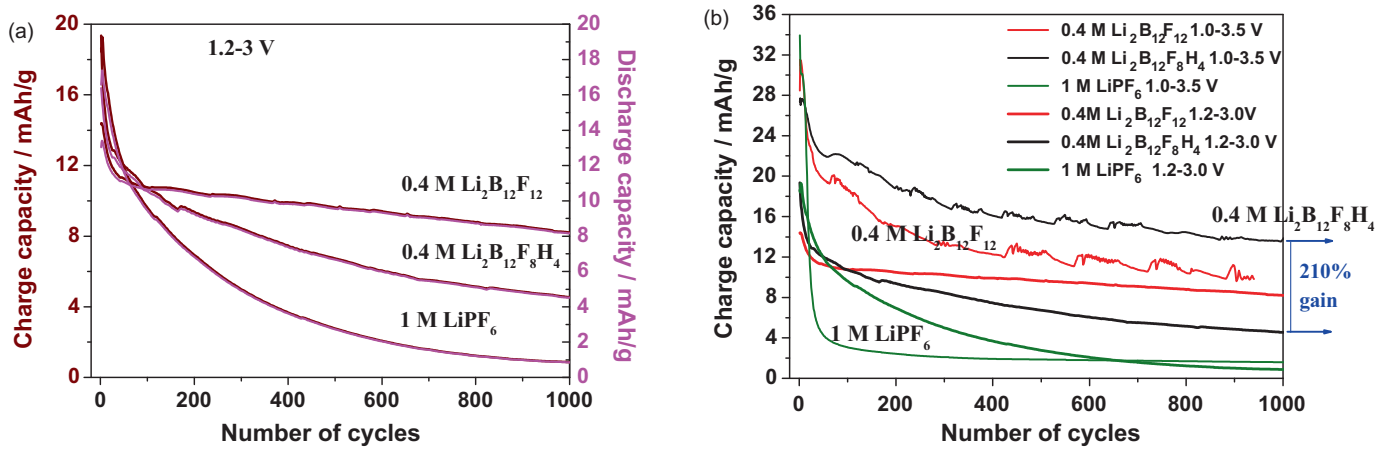

Fig. 6. Cycle life of $Li_4Ti_5O_{12}$/AC cells tested using $Li_2B_{12}F_{12}$ (BF), $Li_2B_{12}F_8H_4$ (BFH) and $LiPF_6$ (LP30) electrolytes between: (a) 1.2–3 V and (b) 1–3.5 V (10C constant charge/discharge rate).

in the high stability, and therefore, higher performances of the cell made using BF or BFH.

According to the total weight of active materials, the cell assembled with $Li_2B_{12}F_{12}$ exhibits energy densities in the range of 20–40 Wh kg^{-1} with power densities in the range of 400–6000 W kg^{-1}. These data have been added to a Ragone plot (Fig. 7) including data from other energy storage devices [19,20]. In such a graph, power density is plotted against energy density, using logarithmic scales in both cases, which allows the comparison of devices having very different characteristics (from extremely low to extremely high power density). In our case, the specific energy and the power were calculated according to:

$$E = C\frac{V_{max}}{m_{total}}$$

and

$$P = V_{max}I$$

where C is the capacity on charge (Ah), V_{max} is the upper limit of the voltage window used durig cycling (V), m_{max} is the total active materials taking into account both electrodes (kg) and I is the imposed current during the galvanostatic charge (10C rate, A).

The cell assembled using BF electrolyte performs very satisfactorily, being able to yield power densities almost equivalent to those obtained with supercapacitors, while the energy density lies in between that of Li-ion batteries and supercapacitors. The energy values obtained for the cells with polyfluorinated boron cluster based salts are comparable to those reported in the literature for other nonaqueous asymmetric supercapacitors using PICACTIF/1 M $LiPF_6$ in EC:2DMC/TiO_2 (45 Wh kg^{-1}) [6] or poly(methyl)thiophene/LTO (58 Wh kg^{-1}) [1], while cell life in our case is enhanced thanks to the redox activity of the electrolyte salt.

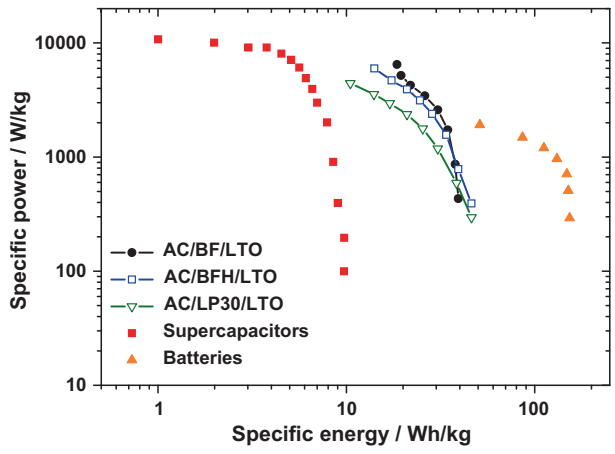

Fig. 7. Ragone plot summarizing the results obtained for cells assembled using $Li_2B_{12}F_{12}$ (BF), $Li_2B_{12}F_8H_4$ (BFH) and $LiPF_6$ (LP30) electrolytes. Data for supercapacitors and batteries (from Refs. [19,20]) are included for comparison.

4. Conclusion

In the present work we have explored the use of novel polyfluorinated boron cluster electrolytes in nonaqueous asymmetric supercapacitors. In all the tests performed, cells assembled with the $Li_2B_{12}F_{12}$ and $Li_2B_{12}F_8H_4$ salts perform better in terms of power and energy density, cyclability and ability to recover initial performances after testing under extreme conditions, as compared to those assembled using the $LiPF_6$-based standard electrolyte. The superior performance of the cells made with these electrolytes is especially important when cycled under harsh conditions, i.e., high discharge rates (up to 150C) or high voltage windows. As is the case in conventional supercapacitors made with the new electrolytes [12], the redox activity of the boron cluster dianions plays a key role in the performance of the devices, acting as a redox shuttle that hinders electrolyte degradation, while at the same time contributing to the capacity delivered. The new salts presented here and, more generally, the $Li_2B_{12}F_xZ_{12-x}$ family, thus represent an exciting alternative to the electrolytes currently used in energy storage devices

Acknowledgements

We acknowledge MATGAS 200 AIE for the provision of their experimental facilities and are grateful to Prof. Pedro Gómez-Romero for helpful discussions. DMR is also indebted to CSIC and the European Social Fund for funding through the I3P program.

References

[1] G.G. Amatucci, F. Badway, A. Du Pasquier, T. Zheng, J. Electrochem. Soc. 148 (2001) A930.
[2] A. Du Pasquier, A. Laforgue, P. Simon, G.G. Amatucci, J.-F. Fauvarque, J. Electrochem. Soc. 149 (2002) A302.
[3] I. Nicotera, G.D. McLachlan, G.D. Bennett, I. Plitz, F. Badway, G.G. Amatucci, S.G. Greenbaum, Electrochem. Solid-State Lett. 10 (2007) A5.
[4] Y.G. Wang, Y.Y. Xia, J. Electrochem. Soc. 153 (2006) A450.
[5] Y.G. Wang, J.Y. Luo, C.X. Wang, Y.Y. Xia, J. Electrochem. Soc. 153 (2006) A1425.
[6] R. Brousse, P.-L. Marchand, P. Taberna, Simon, J. Power Sources 158 (2006) 571.

[7] A. Du Pasquier, I. Plitz, S. Menocal, G.G. Amatucci, J. Power Sources 115 (2003) 171.
[8] A. Du Pasquier, I. Plitz, J. Gural, S. Menocal, G.G. Amatucci, J. Power Sources 113 (2003) 62.
[9] M. Ulman, S.V. Ivanov, W.J. Casteel, G.P. Pez, Polyfluorinated boron cluster anions for lithium electrolytes, US Patent 7311993 (2007).
[10] W.J. Casteel, G. Dantsin, Z. Shi, G. Gopalakrishnan, Abstracts of Papers, 212th Meeting of the Electrochemical Society, Washington, DC, October, 2007 (abstract #725).
[11] C.M. Ionica-Bousquet, D. Muñoz-Rojas, W.J. Casteel, R.M. Pearlstein, G. GirishKumar, G.P. Pez, M.R. Palacín, J. Power Sources 195 (2010) 1479.
[12] C.M. Ionica-Bousquet, W.J. Casteel Jr., R.M. Pearlstein, G. GirishKumar, G.P. Pez, P. Gómez-Romero, M.R. Palacín, D. Muñoz-Rojas, Electrochem. Commun. 12 (2010) 636.
[13] G.J. Wang, J. Gao, L.J. Fu, N.H. Zhao, Y.P. Wu, T. Takamura, Absracts of Papers, International Meeting on Lithium Batteries, Biarritz, France, June, 2006 (abstract #239).
[14] G.J. Wang, J. Gao, L.J. Fu, N.H. Zhao, Y.P. Wua, T. Takamura, J. Power Sources 174 (2007) 1109.
[15] J. Rodriguez-Carvajal, Phys. B 192 (1993) 55.
[16] D. Guyomard, J.M. Tarascon, J. Electrochem. Soc. 139 (1992) 937.
[17] L. Cheng, H.-J. Liu, J.-J. Zhang, H.-M. Xiong, Y.-Y. Xia, J. Electrochem. Soc. 153 (2006) A1472.
[18] T. Ohzuku, A. Ueda, N. Yamamoto, J. Electrochem. Soc. 142 (1995) 1431.
[19] M. Mastragostino, F. Soavi, J. Power Sources 174 (2007) 89.
[20] K. Naoi, P. Simon, Electrochem. Soc. Interface 17 (1) (2008) 34.